JANUARY 2019 | VOL 177 | NO 1

ADVANCED MATERIALS & PROCESSES

AN ASM INTERNATIONAL PUBLICATION

ADVANCED CHARACTERIZATION

AUTOMATED MICROGRAPH ANALYSIS

P.16

ASM INTERNATIONAL

AUTOMATED MICROGRAPH ANALYSIS ENABLES PIONEERING R&D

John Sosa, Pavel Sul, and Lawrence Small,
MIPAR Software, Worthington, Ohio

Advances in software algorithms and design enable automation of microstructure image analysis, leading to cost savings, reduction in measurement variability, and access to important metrics.

Micrograph analysis and characterization is a key function of many materials laboratories supporting manufacturing, quality control, and R&D. While classic methods are subjective and resource intensive, advancements in capture technology along with novel approaches to computer algorithm development enable automated techniques not possible previously. This article discusses the benefits of automated micrograph characterization in scanning electron microscopy (SEM), the necessity of image-based analysis in particle characterization, and challenges in modernizing industry standards.

ALTERNATIVES TO EBSD FOR GRAIN SIZE MEASUREMENT

Grain size is a critical microstructural parameter that directly influences the mechanical properties of nearly all structural materials. Accurate quantification of a material's average grain size and distribution is therefore of paramount importance, as inaccurate measurements can lead to poor quality control, inaccurate property predictions, and inefficient R&D cycles.

Etching procedures do not sufficiently reveal grain boundaries for optical microscopy in some microstructures and grains are too small to be optically imaged in others. In both cases, SEM is often enlisted to image grains. However, the two common SEM imaging modes, i.e., secondary electron (SE) and backscattered electron (BSE) imaging, can produce less grain contrast than optical microscopy, even with proper sample preparation. In these cases, electron backscatter diffraction (EBSD)[1] has historically been the go-to technique for identifying discrete grains for automated analysis. With EBSD, the crystal structure and orientation of each pixel are determined, and these data are subsequently processed to reveal the material's grain structure.

EBSD LIMITATIONS

In some applications, grain orientation data are used to report crystallographic texture in addition to grain size[2]. For this purpose, EBSD is typically an irreplaceable technique. However, EBSD is often used purely for grain size analysis[3], primarily when prior attempts to identify grains using SE and BSE imaging have failed. While EBSD can accurately report grain size, shortcomings of the technique include:

- *Time intensive:* EBSD collection time of a single field-of-view commonly ranges from two to eight hours. High-speed cameras reduce collection time in some applications, but cameras are expensive and even more sensitive to sample preparation and material composition.
- *Limited resolution:* The nature of the electron beam/sample interaction in traditional SEM imaging versus EBSD typically means that SEM imaging can resolve smaller features than EBSD.
- *Tedious sample preparation:* To produce useful data using EBSD, samples must be relatively free of internal strain and their surfaces meticulously polished to a mirror finish with extreme care taken at each step.

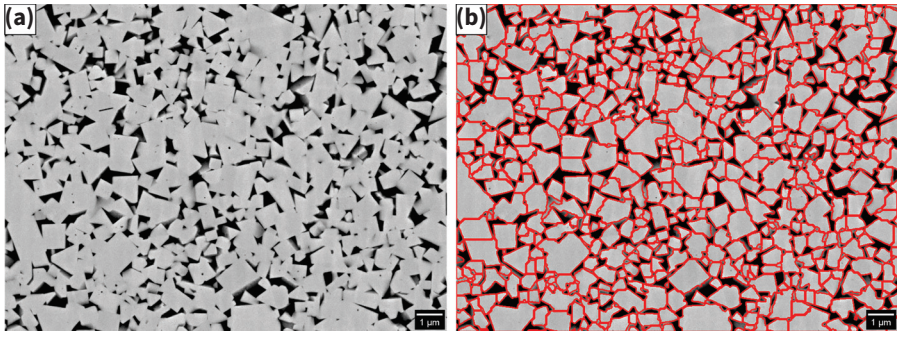

Fig. 1 — (a) Original BSE image; (b) outline of automatically identified grains (red) on original image.

CASE STUDY: REPLACING EBSD FOR GRAIN SIZE ANALYSIS

A manufacturer wanted to replace EBSD grain size measurement with automated BSE SEM image analysis. Figure 1(a) shows an example image of the microstructure of interest. Even with optimal sample preparation, several software solutions failed to detect the microstructure's BSE-imaged grain boundaries with acceptable accuracy. BSE imaging provides an incomplete representation of the microstructure's grain boundaries (Fig. 1a).

Experienced metallographers can mentally connect the dots to delineate each grain, but the task can be very difficult to automate. In this case, the need to connect the dots, together with the faint contrast exhibited by visible boundaries were the primary challenges that previous automated solutions failed to overcome. Recognizing that manual grain analysis from SEM images is no longer feasible nor acceptable, the company was forced to continue with EBSD for automated grain sizing.

The company worked with Mipar Software to pursue automated BSE grain size analysis. A promising automated solution was quickly developed including an adaptive feature detection capability that captures subtle boundary contrast, and a "separate features" function, which mimics human interpretation to complete the partially revealed grain structure. Figure 1(b) shows an outline of the automatically identified grains on the original image.

VALIDATION

To complement the grain detection in Fig. 1(b), Mipar wanted to quantify the accuracy with which grain size could be measured from BSE imaging. Figure 2 compares the raw images, grain detections, and grain size distributions extracted from BSE and EBSD images. Table 1 compares grain size statistics from each method, where statistics and distributions were produced by collecting measurements from four random fields of view. Edge grains were excluded from measurement in each method.

Figure 2 and Table 1 show strong agreement between grain size distributions and summary statistics. BSE mean grain size deviated from that of EBSD by only 2.7%. The standard deviations also show close agreement, but were not strongly considered in the comparison because they, together with maximum and minimum values, are more dependent on the particular fields imaged. A more thorough sampling is required to properly compare standard deviation as well as minimum and maximum statistics between the two. Most importantly, a 97.3% agreement between BSE and EBSD mean grain size delivers confidence in the ability to accurately and automatically perform grain size analysis from BSE images of the challenging microstructure.

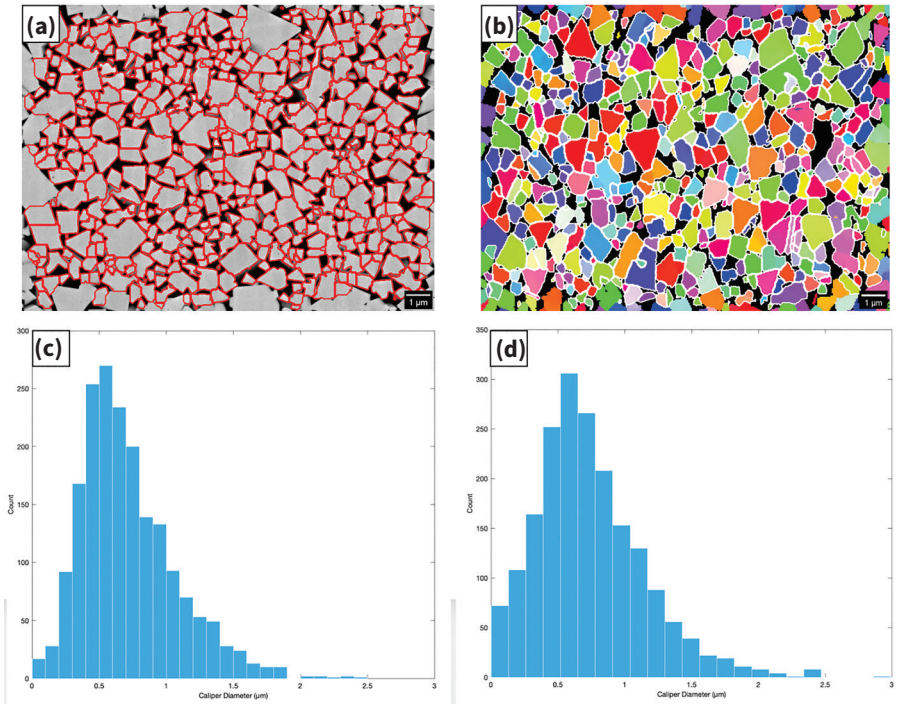

Fig. 2 — (a) Outline of complete identified grains (red) from BSE image; (b) outline of complete identified grains (white) from EBSD image; (c) grain size distribution from four BSE images; and (d) grain size distribution from four EBSD images

TABLE 1 – GRAIN SIZE STATISTICS FROM SEM IMAGING METHODS [a]

	Backscattered electron (BSE)	Electron backscatter diffraction (EBSD)
Mean, µm	0.72	0.74
Standard deviation, µm	0.35	0.41
Minimum, µm	0.04	0.04
Maximum, µm	2.46	3.23

[a] Data from measurements from four random fields of view.

TABLE 2 – TIME AND COSTS FOR BSE AND EBSD GRAIN SIZE ANALYSIS

	Backscattered electron (BSE)	Electron backscatter diffraction (EBSD)
Collection time [a]	50 s/sample	10 h/sample
Samples per day [b]	240	2.4
Estimated SEM rate	$200/h	$200/h
Collection cost per sample [a]	$20/sample	$2000/sample

[a] Assuming five fields per sample. [b] Assuming 24 h SEM access and 5 min sample exchange time.

IMPLICATIONS

Accurate grain size measurement via BSE imaging rather than EBSD offers substantial cost savings and enhanced throughput. Table 2 presents an approximate breakdown of time and service cost associated with each method. Mipar's analysis time of five seconds per image was considered negligible, and is thus excluded from the cost breakdown.

The true cost of grain size data acquisition is more complicated than indicated in Table 2 and likely varies among companies. However, it is not unreasonable to estimate that BSE imaging can offer savings in the thousands of dollars per sample compared with EBSD. Moreover, BSE imaging can conservatively offer 100 times the throughput of EBSD. Thus, while BSE imaging today could potentially process 240 samples in 24 hours with a direct cost of $4800, EBSD would require about four months to process the same volume, with a direct cost of $576,000.

These benefits have been recognized for some time, but the challenges associated with automating grain detection from real-world SEM images forced engineers to resort to EBSD for grain sizing, despite the substantially higher cost. The ability to successfully overcome these challenges enabled Mipar software users to move to BSE grain sizing with significant cost savings and to process samples with greatly increased efficiency.

OVERCOMING MEASUREMENT LIMITATIONS

Powder and loose aggregate materials are used in many engineering applications. Their physical properties determine powder flow characteristics, packing density, composite material properties, and the suitability of aggregates for various purposes. While this variety of properties determines aggregate behavior and suitability for use, many particle assays are restricted to particle size while other important information is lost. Micrograph analysis retains more particle characteristics, enabling more accurate prediction of the aggregate's behavior.

PHYSICAL METHODS

Several techniques are available to characterize particle properties. For granular aggregate materials, the simplest technique to determine particle size distribution is sieve analysis[4,5]. After sifting through meshes of graduated sizes, the percent-by-mass of each size range and a fineness modulus of the material trapped by each sieve is calculated. The technique requires moving samples offline for analysis and it is unable to provide more detailed shape information.

More sophisticated techniques such as acoustic emission avoid some of the limitations of sieve analysis. For example, acoustic emission is rapid, generates a continuous size distribution, and does not require removing samples from the test apparatus[6]. It can measure very small (micron range) particle sizes, but is limited to a maximum particle size. However, like sieve analysis, acoustic emission is limited to size measurements.

Dynamic light scattering, also known as photon correlation spectroscopy[7], is used to make size measurements (down to the nanometer range[8]) of particles in suspension. As particles diffuse through the suspension, they are illuminated by a laser beam and scatter light. Particle size is determined mathematically, which requires assuming particular shape(s), so true shape information is lost.

MICROGRAPH-BASED PARTICLE ANALYSIS

The main benefit of using micrographs to analyze particles over physical techniques is that particle shape information is not lost. Once particles are properly identified in a micrograph, many different shape descriptors such as aspect ratio and roughness can be reported. Using morphological image processing, more complicated analysis can be designed to report metrics such as number of satellite particles per parent, amount of cracking per particle, and many others (Fig. 3). Another benefit of micrograph analysis is that there is no minimum or maximum particle size that can be analyzed. This flexibility requires the use of more powerful and expensive microscopes to achieve smaller resolutions. The basic image processing techniques are not scale dependent.

Micrograph particle analysis, unlike physical techniques, does not require particles to be free to move relative to each other. Particles can be measured as long as they are distinguishable in the image, even if they are fixed in a concretion or composite material, such as after the molding step of a metal injection molding process[9]. This enables further analysis of particle size and shape after production. In addition, measuring particle anisotropy across the image enables investigating nonuniform mechanical properties of the part.

Particle shape information is crucial in powder-based additive manufacturing techniques, as shape characteristics directly influence flow rate and packing density, which in turn influence mechanical and thermal properties of the final product[10].

REDUCING ERRORS IN GRAPHITE CLASSIFICATION

Micrograph analysis is performed to quantify inclusions and porosity in a material using standard reference micrograph charts. However, simply comparing micrographs to a chart is subjective and introduces human error, leading to wrongly approved and rejected parts. Implementing point-counting techniques can reduce some bias, but this increases the time needed to quantify a sample. Also, these techniques do not eliminate the subjectivity inherent in deciding which feature class is under each point. Using a microscope with a digital camera, the micrograph can be digitized as an image and

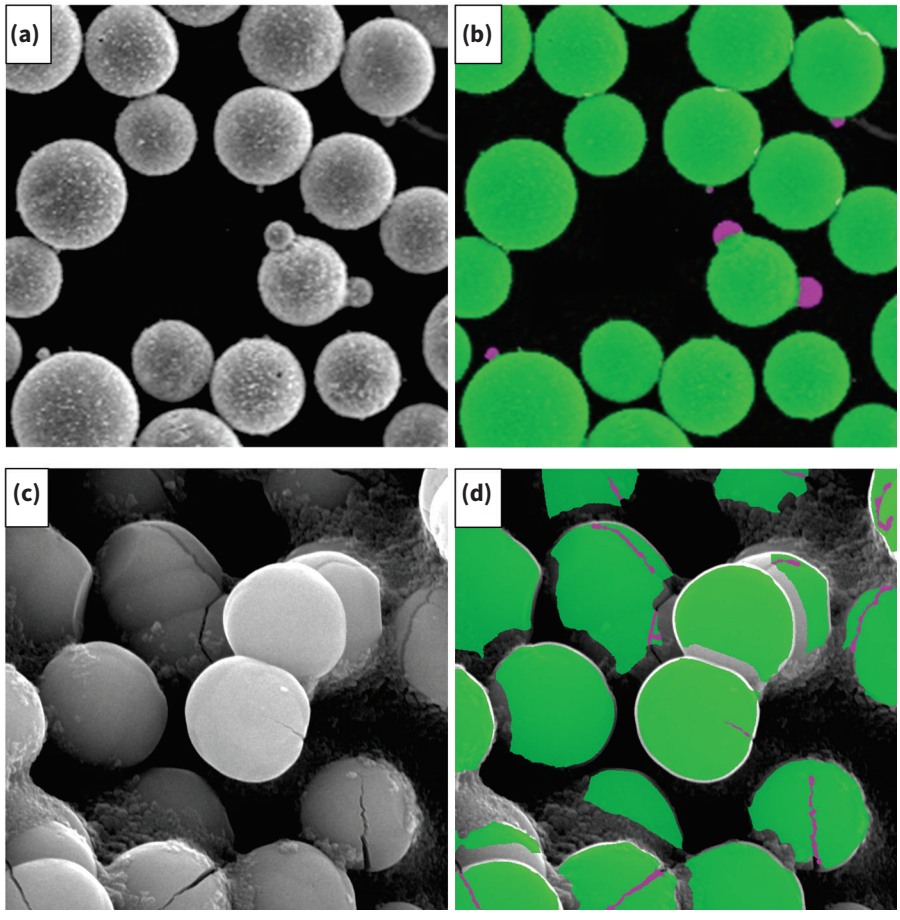

Fig. 3 — Examples of particles and their features identified using Mipar's morphological image processing. (a) Original image of particles with satellites; (b) segmented images (green = parent particles, purple = satellite particles); (c) original image of particles with cracks; and (d) segmented images (green = particles, purple = cracks within those particles).

quantified using a computer algorithm. For example, an algorithm can simulate a point count at every point on an image and apply logic to subclassify material phases, inclusions, and porosity, and generate relevant measurements, all in a matter of seconds. This method provides high speed, high accuracy, and correctable bias.

Technological advancements in microscopes and cameras open the possibility to automate many industry standards for micrograph analysis. Further, advancements in computer algorithms and the introduction of machine learning to this field increase problem solving capabilities. Mipar is working with industry to automate microstructure characterization following both internal and industry standards. Because variability exists in sample preparation, image capture method, and sample characteristics, algorithms are tailored to the user to accommodate inherent variability, but calibration relies on industry standards such as the ASTM A247 nodularity standard test method[11].

ASTM A247 is an example of how a computer automated algorithm can reduce error and highlight shortcomings of ambiguous wall chart analysis. Section 10 of the standard states, "Nodularity is expressed by counting the nodular particles and reporting the results as a percentage of the total amount of graphite present in the microstructure." Some might find it unclear whether the nodular graphite should be counted and reported as a count fraction, or if it should be point counted and reported as an area fraction.

This ambiguity is resolved by calibrating the computer algorithm to the standards chart at three points using both count fraction and area fraction (Fig. 4 and Table 3).

Root-mean-square error analysis shows that area fraction interpretation results in lower overall error (7.22%) than the count fraction method (9.23%), as shown in Table 4. The error analysis also points to inherent error in labeling the standards chart. While reviewing the area fraction results, chart micrographs at 20%, 30%, and 40% nodularity have the greatest absolute error from the algorithm. There are no obvious mistakes in the classification of the nodular graphite (Fig. 5), which highlights a subjective inaccuracy in the chart standard.

The most likely source of error is a combination of mislabeled chart values (as it is unlikely that the values are exactly at 10% intervals) and the

TABLE 3 – ALGORITHM CALIBRATION TO ASTM A247 NODULAR GRAPHITE STANDARDS CHART

Chart	Count fraction, %	Area fraction, %
0	1.06	1.41
50	50.00	51.24
100	98.51	100.00
Root mean square error (RMSE), %	1.06	1.08

TABLE 4 – ALGORITHM ERROR ANALYSIS

Chart	Count fraction, %	Area fraction, %
0	1.06	1.41
10	20.00	17.02
20	23.64	32.40
30	42.34	39.55
40	38.89	53.60
50	50.00	51.21
60	48.45	55.04
70	54.74	64.38
80	75.90	82.00
90	73.13	84.53
100	98.51	100.00
Root mean square error (RMSE), %	9.23	7.22

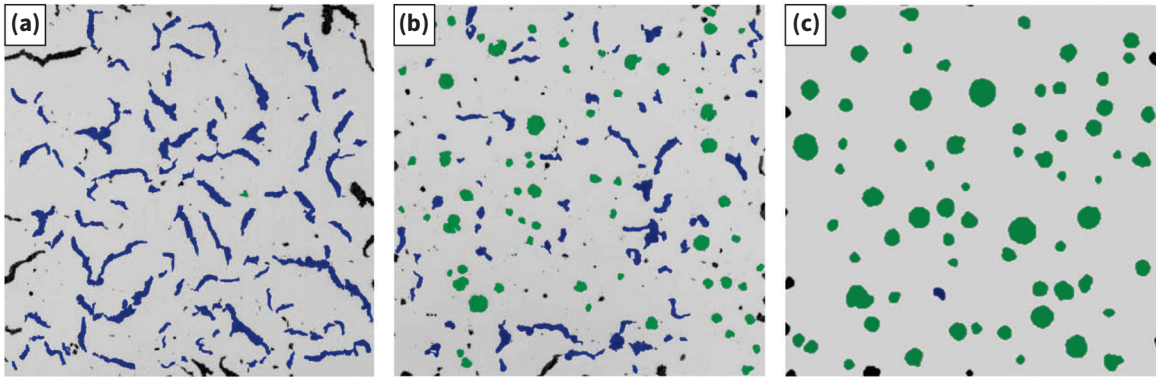

Fig. 4 — Count fraction algorithm calibration results showing ambiguity in ASTM standard reference micrographs for estimating graphite nodularity in ductile iron (see Table 3): (a) 0% nodularity; (b) 50% nodularity; and (c) 100% nodularity (blue = non-nodular graphite and green = nodular graphite).

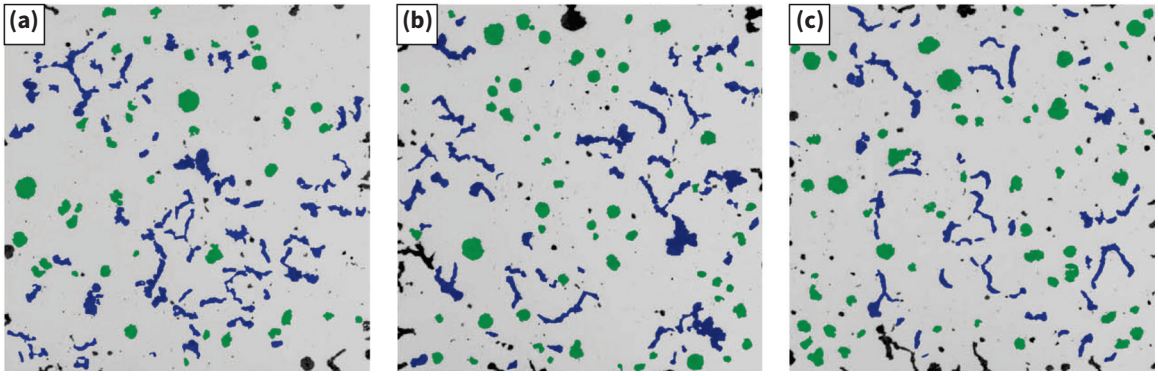

Fig. 5 — Area fraction algorithm error analysis results showing ambiguity in ASTM standard reference micrographs for estimating graphite nodularity in ductile iron (see Table 4): (a) 20% nodularity; (b) 30% nodularity; and (c) 40% nodularity (blue = non-nodular graphite and green = nodular graphite).

subjective nature of micrograph analysis. Additionally, the standard does not provide guidelines for whether graphite on the boundary of the micrograph should be included in the nodularity classification. Nevertheless, the computer algorithm can automate the micrograph analysis while eliminating all random human error. The systematic errors present in automated analysis can be corrected for and further reduced by calibrating the algorithm within a specific range. For example, because ductile iron has a characteristic nodularity of 80-100%, an automated solution can be further calibrated in this range, and then only applied to ductile irons going forward.

As the industry moves toward automation, there is a demand to modernize outdated standards to include guidelines and ground-truth datasets that would allow engineers to work more confidently in the field of material development and characterization. **~AM&P**

For more information: John Sosa is CEO of Mipar Software, 5701 N. High St., Suite 204, Worthington, OH, 43085, 614.407.4510, support@mipar.us, www.mipar.us.

References

1. M.N. Alam and M. Blackman, High-Angle Kikuchi Patterns, *Proc. Royal Soc. of London A: Mathematical, Physical and Engineering Sciences*, *221*(1145), p 224-242, 1954.

2. D.J. Dingley and V. Randle, Micro-texture Determination by Electron Backscatter Diffraction, *J. Matls. Sci., 27*(17), p 4545-4566, 1992.

3. F.J. Humphreys, Characterization of Fine-Scale Microstructures by Electron Backscatter Diffraction (EBSD), *Scripta Mater., 51*(8), p 771-776, 2004.

4. Standard Test Method for Sieve Analysis of Fine and Coarse Aggregates, ASTM C136/C136M-14, ASTM, 2014.

5. Standard Specification for Woven Wire Test Sieve Cloth and Test Sieves, ASTM E11-17, ASTM, 2017.

6. E. Nsugbe, et al., Monitoring the Particle Size Distribution of a Powder Mixing Process with Acoustic Emissions: A Review, *Eng. Technol. Ref.,* p 1-12, 2016.

7. Standard Guide for Measurement of Particle Size Distribution of Nanomaterials in Suspension by Photon Correlation Spectroscopy (PCS), ASTM E2490-09, ASTM, 2015.

8. R. Pecora, Dynamic Light Scattering Measurement of Nanometer Particles in Liquids, *J. Nanopart. Res.,* 2, p 123-131, 2000.

9. D.F. Heaney and C.D. Green, Molding of Components in Metal Injection Molding (MIM), in D.F. Heaney (Ed.), *Handbook of Metal Injection Molding,* Woodhead Publishing Ltd., Cambridge, UK, 2012.

10. J.M. Benson, et al., The Need for Powder Characterization in the Additive Manufacturing Industry and the Establishment of a National Facility, *S. Afr. J. Ind. Eng.,* 26, p 104-114, 2015.

11. Standard Test Method for Evaluating the Microstructure of Graphite in Iron Castings, ASTM A247-17, ASTM, 2017.